Published in final edited form as:
J Cell Physiol. 2010 April ; 223(1): 76. doi:10.1002/jcp.22012.

RANKL induces heterogeneous DC-STAMP^{lo} and DC-STAMP^{hi} osteoclast precursors of which the DC-STAMP^{lo} precursors are the master fusogens

Kofi A. Mensah, PhD[1,2], **Christopher T. Ritchlin, MD,MPH**[1,3], and **Edward M. Schwarz, PhD**[1,4]

[1]Center for Musculoskeletal Research, University of Rochester Medical Center, Rochester, NY, USA

[2]Department of Microbiology and Immunology, University of Rochester School of Medicine and Dentistry, Rochester, NY, USA

[3]Allergy, Immunology & Rheumatology Unit, Department of Medicine, University of Rochester Medical Center, Rochester, NY, USA

Abstract

Osteoclasts (OC) are multinucleated bone resorbing cells that form via RANKL-induced fusion of heterogeneous mononuclear OC precursors (OCP). Currently, there are no unique surface markers to distinguish these OCP populations, which are diagnostic for erosive and metabolic bone diseases using culture assays. Thus, we investigated expression of DC-STAMP, a surface receptor required for OCP fusion, during osteoclastogenesis *in vitro* using a novel monoclonal antibody (1A2). Immunoprecipitation-western blot analysis of OCP membrane proteins detected 106 kDa dimeric and 53 kDa monomeric DC-STAMP in non-denaturing and denaturing conditions respectively, with greater sensitivity vs. rabbit anti-sera (KR104). 1A2 also detected 99.9% of undifferentiated monocytes as a single population by flow cytometry with a MFI 100-fold over background, while KR104 was not useful in this assay. Functionally, 1A2 inhibited OCP fusion *in vitro*. RANKL stimulation of OCP induced DC-STAMP^{lo} and DC-STAMP^{hi} cells, which mature into OC and mononuclear cells respectively as determined by fluorescent microscopy and TRAP assays. Addition of DC-STAMP^{hi} cells to purified DC-STAMP^{lo} cultures produced larger, more nucleated OC vs. pure DC-STAMP^{lo} cultures. RT-qPCR analysis of these two populations showed that OC markers (*Trap* and *Oc-stamp*) and fusogenic gene expression (*Cd9* and *Cd47)*, were significantly increased in DC-STAMP^{lo} vs. DC-STAMP^{hi} cells. Collectively, these results demonstrate that DC-STAMP is expressed on OCP as a dimer, which is efficiently detected by 1A2 via flow cytometry. RANKL induces osteoclastogenesis by stimulating DC-STAMP internalization in some OCP, and these DC-STAMP^{lo} cells display the “master fusogen” phenotype. In contrast, DC-STAMP^{hi} OCP can only act as mononuclear donors.

Keywords

Dendritic Cell-Specific Transmembrane Protein (DC-STAMP); Osteoclast Precursors (OCP); Cell Fusion

4To whom correspondence should be addressed: The Center for Musculoskeletal Research University of Rochester Medical Center 601 Elmwood Avenue, Box 665, Rochester, NY 14642 Phone 585-275-3063, FAX 585-756-4727 Edward_Schwarz@URMC.Rochester.edu..

Introduction

Osteoclasts (OC) are multinucleated giant cells derived from monocyte-lineage haematopoietic cells, and are uniquely designed to resorb bone (Teitelbaum, 2000). A pivotal event in OC development is multinucleation, which takes place when mononuclear OC precursors (OCP) fuse with one another to form polykaryons (Boyle et al., 2003). This process is analogous to the fusion events that take place between macrophages to form giant cells, and involves the coordinated activity of several adhesion molecules, fusion proteins, and regulators of this process (Vignery, 2005). While several ubiquitous proteins that regulate mammalian cell fusion have been identified (i.e. CD9, CD47, CD44, and SIRPα) (Chen et al., 2007; Hayer et al., 2005; Ishii et al., 2006; Lundberg et al., 2007), dendritic cell-specific transmembrane protein (DC-STAMP) appears to be specific and critical for osteoclastogenesis and giant cell formation (Kukita et al., 2004; Yagi et al., 2005; Yagi et al., 2006; Yagi et al., 2007). DC-STAMP was initially identified in myeloid dendritic cells as a 53 kDa, interleukin-4 (IL-4)-inducible protein consisting of seven transmembrane domains with no considerable sequence homology to other proteins (Hartgers et al., 2000). DC-STAMP has also been found in macrophages and OC (Yagi et al., 2005). In OC, DC-STAMP is essential for multinucleation in the presence of RANKL and M-CSF (Yagi et al., 2005). Recent studies with mice genetically deficient for DC-STAMP suggest a critical role in OCP fusion since these mice have few multinucleated TRAP+ OC and increased bone mineral density (Kukita et al., 2004; Yagi et al., 2005; Yagi et al., 2006; Yagi et al., 2007). Conversely, experiments in DC-STAMP-Tg mice revealed accelerated bone resorption and concomitant decreased bone mass (Iwasaki et al., 2008). OCP from DC-STAMP$^{+/+}$ mice have been shown to be capable of fusing with OCP from DC-STAMP$^{-/-}$ mice suggesting a heterotypical nature for the role of DC-STAMP in osteoclastogenesis (Yagi et al., 2005).

We hypothesize that regulation of the DC-STAMP surface protein expression pattern is critical during osteoclastogenesis, and that this protein expression pattern determines which OCP have the greatest fusogenic and thus osteoclastogenic potential. Previous studies have greatly added to our knowledge about the differential regulation of DC-STAMP during osteoclastogenesis; however, the previously reported assays focused mainly on gene expression and do not study specific, endogenous DC-STAMP protein levels. Furthermore, the methods employed in those initial analyses are complex and may not be easily adaptable to application in clinical settings where flow cytometry can evaluate differences between cell types based on surface and intracellular protein expression patterns. To-date, direct assessment of the temporal DC-STAMP protein expression pattern during differentiation of monocyte/macrophage precursor cells into OC has not been reported, likely due to the absence of reagents to detect the native molecule (i.e. monoclonal antibodies (mAb)). Thus, we generated a novel anti-DC-STAMP mAb (1A2) and used it for flow cytometry analysis of the RAW 264.7 murine monocyte/macrophage cell line, and primary murine bone marrow macrophages. With the 1A2 mAb we investigated DC-STAMP protein expression during osteoclastogenesis to phenotype the early OCP and determine if there is heterogeneity that allows them to be categorized based on their roles in the fusion process.

Another important aspect of OCP biology is it role in erosive arthritis (Schwarz et al., 2006). Previously, we demonstrated that psoriatic arthritis patients have a significant increase in circulating OCP frequency vs. healthy controls, and that the increase correlated with radiographic progression and amelioration with effective anti-TNF therapy (Anandarajah et al., 2008; Ritchlin et al., 2003). Subsequently, others have used these tedious *in vitro* culture assays to study OCP frequency as a diagnostic marker of erosive disease in patients with osteoporosis, rheumatoid arthritis, spondyloarthropathy, and tophaceous gout (Dalbeth et al., 2008; Nose et al., 2009; Vandooren et al., 2009). Although circulating OCP frequency holds

promise as a clinical biomarker for erosive disease, the absence of a facile, rapid diagnostic markedly limits its potential.

Materials and Methods

Animals

C57Bl/6 mice were purchased from JAX Mice and Services, Bar Harbor, ME, USA. The mice were handled in accordance with protocol approved by the Institutional Animal Care and Use Committee of the University of Rochester (Rochester, NY, USA).

Isolation and culture of cells to generate OC

Mouse bone marrow cells were obtained aseptically as previously described (Takeshita et al., 2000), by flushing the femora and tibiae of 20-week-old C57BL/6 mice with sterile 1X phosphate-buffered saline (PBS). Red blood cells in the collected suspension were lysed with ammonium chloride solution (Stem Cell Technologies), and the collected cells were cultured in minimal essential media- alpha modification (alpha-MEM) (Invitrogen, Carlsbad, CA, USA), supplemented with 10% heat-inactivated fetal calf serum, 5% penicillin / streptomycin, and 5% minimal essential medium nonessential amino acids (Invitrogen) with a final pH of 7.4. The cells were incubated at 37 °C in 5% CO_2 atmosphere. M-CSF (50 ng/mL) was added to the bone marrow-derived cells for 3 days to enrich the adherent CD11b+ (Mac-1+) population as previously described (Hayashi et al., 2002). After 3 days, 100 ng/mL RANKL (Cell Sciences, Canton, MA) in alpha-MEM was added to the cells for 3 more days to generate OC. RAW 264.7 cells or RAW 264.7 GFP cells were treated with 100 ng/mL RANKL in alpha-MEM for 3 days to generate OC.

RNA analysis

Total RNA was extracted from the cells using the Qiagen RNeasy mini kit (Qiagen, Valencia, CA, USA) and subsequently reverse-transcribed into cDNA using the iScript cDNA synthesis kit (BioRad, Hercules, CA, USA). Real-time PCR reactions were performed in triplicate using the Rotor-Gene 3000 thermal cycler (Corbett Life Science, Sydney, NSW, Australia). The RT^2 qPCR Primer Assay for mouse *Dc-stamp* (Superarray, Frederick, MD, USA) was used for PCR analysis. As in previous reports (Yagi et al., 2007), *β-actin* served as the internal house-keeping gene control (forward primer sequence 5′-AGATGTGGATCAGCAAGCAG-3′, reverse primer sequence 5′-GCGCAAGTTAGGTTTTGTCA-3). SYBR Green I (Applied Biosystems, Foster City, CA, USA) was used for detection of DNA synthesis under the following cycling conditions: 95 °C, 10 min followed by 45 cycles of 95 °C, 15 sec; 60 °C, 60 sec; 72 °C 15 sec. The amount of *Dc-stamp* mRNA expressed was normalized to the *β-actin* expression for the specific treatment condition.

For OC markers and fusion-related genes, the following table depicts the various primers used and their annealing temperatures:

Gene	Primer Sequences (F: forward sequence, R: reverse sequence)	Annealing Temperature (°C)
Trap	F: 5′-CAGCTGTCCTGGCTCAAAA-3′ R: 5′-ACATAGCCCACACCGTTCTC-3′	54
Rank	F: 5′-ACCATCCAGCTGTCTTCCCCA-3′ R: 5′-TTACTGTTTCCAGTCACGTTCCCAGAGG-3′	57
Trem2	F: 5′-TGAGCCTGACTGGCTTGGTCA-3′ R: 5′-ACCATCCAGCTGTCTTCCCCA-3′	57
Cd9	F: 5′-CTTGCTATTGGACTATGGCT-3′ R: 5′-GTCCGAGATAAACTGCTCCA-3′	59
Cd44	F: 5′-TAGGAGAAGGTGTGGGCAG-3′ R: 5′-AGGCACTACACCCCAATC-3′	50

Cd47	F: 5′-AGATGTGGCCCTTGGCG-3′ R: 5′-TGCTCAGACAACTGTATTC-3′	50
Sirpα	F: 5′-TCGAGTGATCAAGGGAGCAT-3′ R: 5′-CCTGGACACTAGCATACTCTGAG-3′	59
Oc-stamp	F: 5′-TGGGCCTCCATATGACCTCGAGTAG-3′ R: 5′-TCAAAGGCTTGTAAATTGGAGGAGT-3′	54

Antibody development

A monoclonal antibody against DC-STAMP was generated by immunizing mice with a fifteen amino-acid peptide sharing homology to a sequence in the fourth extracellular domain of both murine and human DC-STAMP. Hybridoma clones with strong signals by EIA generated by this immunization procedure were expanded in SAFC EX-CELL 610 HSF serum-free media (Sigma, St. Louis, MO, USA) and used to generate antibody, which was purified using HiTrap protein G and PD10 columns (GE Healthcare Biosciences, Piscataway, NJ, USA). The 1A2 clone from this process was evaluated and used for all analyses in this study. Conjugation to FITC was performed using the Molecular Probes labeling kit (Invitrogen).

Immunoprecipitation-western blot (IP-western)

The anti-DC-STAMP monoclonal antibody (mAb) was used to immunoprecipitate DC-STAMP from cells treated with RANKL for 2 days. The Native Membrane Protein Extraction Kit (Calbiochem, San Diego, CA, USA) was used to extract membrane fraction proteins according to the manufacturer's instructions. The extracted membrane fraction proteins were immunoprecipitated using the EZView Red Protein A Affinity Gel beads (Sigma) after incubation for 1 hour at 4 °C with anti-DC-STAMP mAb to form antibody-antigen complexes.

Following immunoprecipitation, immunoblotting was done using by loading the immunoprecipitated protein onto a 10% gel for SDS-PAGE. The separated proteins were blotted onto a PVDF membrane using a wet-transfer method. After transfer, the membrane was blocked for 1 hr at room temperature with 5% BSA (Sigma) in TBST. Then, either the anti-DC-STAMP mAb clone 1A2, commercially-available rabbit anti-mouse DC-STAMP polyclonal antibody KR104 (Cosmo Bio, Tokyo, Japan), or mouse IgG (Caltag, Burlingame, CA, USA) was added at a 1:1000 dilution in the blocking solution overnight at 4 °C. Following washes in TBST, goat anti-mouse IgG horse-radish peroxidase conjugate (BioRad) was added at a 1:3000 dilution, followed by more TBST washes. The blots were developed with the SuperSignal West Femto chemiluminescent substrate kit (Pierce, Rockford, IL, USA) and imaged on Kodak scientific films (Eastman Kodak, Rochester, NY, USA).

Flow cytometry

RAW cells and murine bone marrow macrophages were stained in the dark on ice with FITC-conjugated anti-DC-STAMP mAb for 30 min in 1X PBS containing 4% FCS after adding anti-CD16/CD32 to block Fc-receptors (BD Pharmingen, San Jose, CA, USA) for 15 min. 7AAD (Invitrogen) was also added to cells during the 30 min incubation, and it was used to determine which cells to gate for subsequent analysis of DC-STAMP surface protein expression. Permeabilization of the cells for intracellular staining was performed using the Cytofix/Cytoperm kit (BD Biosciences Pharmingen). If cells could not be analyzed the same day, they were fixed in 1% PFA and analyzed the following day. Flow cytometry was performed using a FACSCalibur (Becton Dickinson), FACS was performed on the same day of staining using either a FACS Vantage (Becton Dickinson) and data analysis was done with WinMDI 2.9 software (Scripps Research Institute, La Jolla, CA, USA).

Immunofluorescent staining

Murine bone marrow macrophages cultured on glass coverslips in 12-well dishes with 100 ng/mL RANKL. Cells were fixed in 4% PFA for 20 min at room temperature for immunofluorescent staining. The cells were then blocked and permeabilized with PBS containing 0.2% BSA and 0.1% saponin for 15 min. The coverslips were incubated at room temperature for 2 hr in a humid chamber with 1A2 anti-DC-STAMP mAb. After 2 hr, PE secondary antibody, DAPI, or phalloidin was added for 45 min at room temperature in the blocking and permeabilization solution. Following the incubation, the coverslips were washed with PBS and mounted on slides for imaging. Images were then assembled, pseudo-colored, and overlaid using Adobe Photoshop 7.0 software (Adobe Systems, San Jose, CA, USA).

TRAP assays.

Statistical Analysis

Data are presented as means ± standard error of the mean. Student's *t*-test or analysis of variance (ANOVA) were performed with a significance level of $P<0.05$. Statistics were calculated using either Microsoft Excel 9.0 software (Microsoft, Redmond, WA, USA) or the GraphPad PRISM software package (GraphPad Software, La Jolla, CA, USA).

Results

A novel monoclonal antibody to detect DC-STAMP surface expression on OCP

Though DC-STAMP has been shown to be essential to osteoclastogenesis, no studies have examined DC-STAMP surface protein expression by flow cytometric immunophenotyping of cells capable of generating OC. Earlier studies of DC-STAMP protein expression have relied on the use of polyclonal antibodies or antibodies to GFP-tagged DC-STAMP constructs (Eleveld-Trancikova et al., 2005; Kukita et al., 2004; Staege et al., 2001). To specifically study native surface protein expression, we generated a murine mAb to DC-STAMP (1A2). For comparison, we used a commercially available rabbit polyclonal anti-DC-STAMP antibody (KR104), which has histologically shown surface expression on OC (Kukita et al., 2004). In our initial characterization studies, we compared 1A2 versus KR104 in IP-western assays of membrane protein extracts from RANKL stimulated RAW 264.7 cells. Both antibodies recognize a single protein moiety of ~53 kDa and ~106 kDa under reducing and non-reducing conditions respectively and the 1A2 anti-DC-STAMP mAb showed stronger detection of signal for the same amount of protein loaded in each lane (Figure 1A).. Similar results were obtained using protein extracts from human PBMC (data not shown). These data indicated that DC-STAMP is expressed as a dimer on the plasma membrane of murine and human OCP, and is specifically recognized by 1A2.

Having demonstrated that both the 1A2 and the KR104 recognize the 53 kDa DC-STAMP by IP-western blot (albeit to different degrees), we compared their ability to recognize surface DC-STAMP by flow cytometry. Figure 1B shows that the 1A2 mAb recognized homogeneous expression of DC-STAMP on the surface of RAW 264.7 cells cultured in plain media. Virtually 100% of the RAW cells are surface DC-STAMP+ and have a strong mean fluorescence intensity (113.4). By contrast, KR104 was unable to detect this level of DC-STAMP among the RAW cells, as only 21% of the RAW cells appear surface DC-STAMP+ and with a low MFI (14.7). When looking at the signal obtained with the secondary goat anti-rabbit antibody (dotted line), it is apparent that the majority of the KR104 signal is background.

Finally, we evaluated the functional effects of 1A2 *in vitro* using TRAP osteoclastogenesis assays to see if the mAb inhibits RANKL-induced OCP fusion compared to that previously described with KR104 (Kukita et al., 2004). Figure 1C-F demonstrate that 1A2 dose-

dependently inhibited OC formation of RANKL stimulated RAW cells and murine bone marrow macrophages.

RANKL induces two populations of OCP defined by their surface DC-STAMP expression profile

We treated bone marrow cells from C57Bl/6 mice with M-CSF for 3 days to enrich for the monocyte/macrophage CD11b+ population as previously described (Takeshita et al., 2000). We then treated these cells with RANKL for three more days. After 3 days of culture with RANKL, we harvested the cells for flow cytometry to detect surface and intracellular DC-STAMP expression. We observed that there is a strong single peak expressed very homogeneously in untreated cells (Figure 2A – dotted line histogram). After 1 day of RANKL culture, there was still a single peak expressed fairly homogeneously among the cells, but a slight downward shift in the mean fluorescence intensity was noted (Figure 2A). On day two of culture with RANKL, the percentage of cells expressing the day-one level of surface DC-STAMP began to decline further to 62%, while a second population of DC-STAMP^{lo} was visible. After 3 days of RANKL culture, this population of RANKL-induced DC-STAMP^{lo} cells was the predominant cell type, and only 45% of the original level of pre-culture levels of DC-STAMP was observed. This RANKL-induced heterogeneity was dose-dependent, as proportionally lower numbers of DC-STAMP^{lo} cells were generated after 3 days of culture with 10-fold less cytokine (Figure 2G).

To examine the mechanism responsible for the shift in surface DC-STAMP expression, we used the forward and side scatter parameters to specifically identify and gate permeabilized cells and to measure intracellular levels of DC-STAMP inside the permeabilized OCP over the same period of time and under identical culture conditions (Figure 2D). The data revealed that a low percentage of cells expressed intracellular DC-STAMP after 1 day of culture with RANKL. By day two, when surface DC-STAMP levels began to decline and the RANKL-induced DC-STAMP^{lo} cells began to appear, the intracellular DC-STAMP levels also rose to 6.6%. By day three, when the predominant cell type in culture was DC-STAMP^{lo}, and TRAP + multinucleated OC were visible in the culture dish, the intracellular DC-STAMP levels were 18.3%.

To confirm this shift in DC-STAMP cellular localization, we performed immunofluorescence microscopy on RAW cells cultured with RANKL for different periods of time. After culture with RANKL for 2 days, RAW cells underwent morphologic changes characteristic of cells early in the process of osteoclastogenesis (Takeshita et al., 2000). These cells expressed intracellular DC-STAMP, which did not co-localize with cortical actin (Figure 3A). After 3 days, when multinucleated cells were abundant in culture, the master fusogens and OC dramatically down-regulated DC-STAMP protein levels, while the mononuclear cells retained high surface DC-STAMP expression that co-localized with cortical actin (Figure 3B). Similar results were obtained with RANKL stimulated cultures of human PBMC from healthy controls (data not shown). To quantify this difference in intracellular DC-STAMP levels, we sorted surface DC-STAMP^{lo} and DC-STAMP^{hi} RAW cells after RANKL exposure for 3 days, and assessed the mean fluorescence intensity (MFI) of permeabilized cells stained with FITC-1A2. The results demonstrated that DC-STAMP^{lo} cells have intracellular DC-STAMP levels that are 3-fold greater vs. DC-STAMP^{hi} cells (Figure 3C). Collectively, these results are consistent with a model of osteoclastogenesis in which some OCP respond to RANKL by internalization of surface DC-STAMP, following ligation with a DC-STAMP ligand and become master fusogens. In contrast, OCP resistant to this signal and remain DC-STAMP^{hi} mononuclear OCP donors

RANKL induced DC-STAMP^{lo} and DC-STAMP^{hi} cells have distinct osteoclastogenic potential

To further investigate RANKL-induced OC formation via DC-STAMP^{hi} and DC-STAMP^{lo} populations, we investigated the osteoclastogenic potential of these two subsets *in vitro*. First, RAW cells were cultured with RANKL for 3 days to generate the two populations (Figure 4A), which were sorted based on DC-STAMP expression, recultured in RANKL for 3 and both individual cells and mixed cultures were stained with TRAP.. The results from the homogenous cultures demonstrated that only DC-STAMP^{lo} cells can form TRAP+ multinucleated OC (Figure 4B), while culture of RANKL-induced DC-STAMP^{hi} cells alone yielded no TRAP+ multinucleated OC (Figure 4C). A 10:1 ratio of DC-STAMP^{lo}:DC-STAMP^{hi} cells gave rise to larger and more multinucleated OC (Figure 4D). Interestingly, the limited OC formation that was observed in the pure DC-STAMP^{lo} cell cultures was not increased by addition of an equal number of DC-STAMP^{hi} cells (Figure 4E), and a 10:1 ratio of DC-STAMP^{hi}:DC-STAMP^{lo} cells failed to produce any large, multinucleated, TRAP+ OC (Figure 4F). Our interpretation of this result is that the large OC form via DC-STAMP^{lo} master fusogen acquisition of DC-STAMP^{hi} OCP donors, and that homotypic cell fusion is very inefficient.

RANKL-induced DC-STAMP^{lo} OCP express higher levels of OC marker and fusion-related genes

Next, we looked for differences in expression of master fusogen marker gene mRNA levels between the two populations, which were generated from RANKL stimulated RAW cells, and normalized the data to mRNA levels in unstimulated RAW cells (Figure 5). First we analyzed *Dc-stamp* mRNA levels, which were significantly lower by 60% in DC-STAMP^{hi} cells compared to baseline levels in unstimulated RAW cells (Figure 5A).

Gene expression profiling for *Rank* and *Trem2* showed no statistically significant differences between RANKL-induced DC-STAMP^{hi} OCP and RANKL-induced DC-STAMP^{lo} OCP. In fact, *Rank* expression was decreased in both populations by an average of 98% (Figure 5B). Interestingly, and in support of the *in vitro* osteoclastogenesis results, *Trap* expression was significantly greater by 11.3 fold in RANKL-induced DC-STAMP^{lo} cells (Figure 5B), which is also consistent with DC-STAMP signaling being directly involved in the induction of TRAP as previously described (Yagi et al., 2005). We also examined the expression of *Oc-stamp*, which was recently described as essential to OC differentiation (Yang et al., 2008). We found a 21-fold increase in the expression of *Oc-stamp* in the RANKL-induced DC-STAMP^{lo} OCP, while only about a 5-fold increase in the RANKL-induced DC-STAMP^{hi} group (Figure 5B). We also analyzed *Cd47, Sirpα, Cd44, and Cd9* gene expression, which are fusogenic molecules shown to be induced by DC-STAMP signaling (Hayer et al., 2005). Transcript levels for *Cd9* and *Cd47* were significantly up-regulated 1.5- and 1.9- fold, respectively, in the DC-STAMP^{lo} population, and were down-regulated or unchanged in the DC-STAMP^{hi} cells. *Sirpα* mRNA levels were significantly more up-regulated in the RANKL-induced DC-STAMP^{hi} population. This is of note because gene expression of its ligand, *Cd47*, was higher in the DC-STAMP^{lo} group. Interestingly, *Cd44* levels were significantly higher in DC-STAMP^{hi} cells (Figure 5B), which is consistent with its role as an inhibitor of cell fusion (de Vries et al., 2005). Collectively, these results demonstrate that DC-STAMP^{lo} cells express higher levels of mature OC and fuseogenic genes, which is consistent with the master fusogen phenotype.

Discussion

Although it has been long known that the large multinucleated OC, which are responsible for metabolic bone diseases and aggressive focal bone loss in erosive arthritis, are formed by cellular fusion of a heterogeneous population of OCP (Goldring and Gravallese, 2000), no surface markers have been identified that can distinguish the master fusogens from the

mononuclear donors. Identification of surface markers that are specific for terminally differentiated OCP is critical to our understanding of OC fusion and blood-based diagnostics to assess a patient's erosion potential. The pan-surface markers that are most commonly used to identify OCP populations (e.g. CD11b, CD14) (Jacquin et al., 2006; Li et al., 2004), are unspecific because they also detect monocytes and DC (Heinemann et al., 2000; Rivollier et al., 2004). To this end we have chosen to investigate DC-STAMP expression, which has recently gained attention for its role in the irreversible events of OC fusion (Vignery, 2005; Yagi et al., 2005; Yagi et al., 2006; Yagi et al., 2007). As a critical tool for these investigations, here we describe the first mAb able to specifically detect DC-STAMP and sort OCP populations based on cell surface expression by flow cytometry.

In the current paradigm RANKL stimulation of homogenous OCP induces the expression of a yet to be identified soluble and/or membrane bound DC-STAMP-ligand, which subsequently induces fusogenic gene expression via autocrine and/or paracrine via G-protein-coupled receptor (GPCR) signaling (Vignery, 2005). Here we present novel findings that largely support this model including: 1) the native form of DC-STAMP is a dimer (Figure 1A), which is consistent with its predicted function as a GPCR (Milligan, 2004); and 2) RANKL-induced fusogenic gene expression is secondary to DC-STAMP signaling (Figure 5). However, the central finding in this study is that RANKL induces heterogeneous OCP that are functionally distinct such that DC-STAMP^{hi} cells are mononuclear donors that cannot form OC by themselves, and DC-STAMP^{lo} cells act as master fusogens (Figure 4). In contrast to the current model, we also demonstrated that surface DC-STAMP expression is not induced by RANKL, as 1A2 staining of OCP is at its peak prior to stimulation (Figures 2). Additionally, our finding that RANKL down-regulation of DC-STAMP on the plasma membrane is coincident with an increase in cytoplasmic DC-STAMP (Figures 2 & 3) is consistent with GPCR endocytosis following ligand binding (Milligan, 2004), and suggests that the function of RANKL-induced *Dc-stamp* mRNA levels (Yagi et al., 2005) is to sustain expression of the receptor in DC-STAMP^{lo} cells during increased protein turnover. Moreover, our data predict that RANKL-induced DC-STAMP^{hi} cells are refractory to DC-STAMP ligand, as they fail to internalize their receptor; downregulate *Dc-stamp* mRNA expression; and do not express high levels of certain fusogenic genes shown to be important in osteoclastogenesis compared to their RANKL-induced DC-STAMP^{lo} counterparts. Elucidation of the mechanism by which DC-STAMP is stabilized on these mononuclear OCP donors is an important future direction towards our understanding of osteoclastogenesis.

The recent development of very potent anti-osteoclastic drugs (zoledronate, denosumab) (Cohen et al., 2008; Jarrett et al., 2006), may overcome the limitations of standard bisphosphonates (alendronate, residronate, etidronate, pamidronate) that are ineffective in preventing focal erosions in patients with inflammatory arthritis (Eggelmeijer et al., 1994; Ralston et al., 1989; Valleala et al., 2003). As a result, there is potential to prevent irreversible joint destruction, and the development of accurate diagnostics is needed to justify the costs and risks associated with these novel therapies. We first described circulating OCP as a biomarker of erosive arthritis based on their elevated levels in psoriatic arthritis patients with radiographic findings, and their normalization with effective anti-TNF therapy (Anandarajah et al., 2008; Ritchlin et al., 2003). While others have also used this approach to assess erosive potential, the utility of OCP frequency as a diagnostic is markedly limited by the tedious and finicky culture assays (Dalbeth et al., 2008; Nose et al., 2009; Vandooren et al., 2009). Thus, our demonstration that 1A2 can be used to phenotype two classes of OCP with different osteoclastogenic potential identifiable by their DC-STAMP surface expression pattern opens new doors in the field of bone biology and supports the long-suspected idea of cellular heterogeneity during the fusion process. The ability to separate these cells and study their roles in OCP fusion will enable studies that provide new insight about how pro- and anti-osteoclastogenic factors influence this process. This finding not only has the capacity to further our understanding of

osteoclastogenesis but can aid in the development of new therapeutic targets for erosive bone diseases. A larger clinical study is warranted to confirm these initial findings with radiographic progression data, and cell sorting experiments to authenticate the use of the percentage of DC-STAMP^{lo} PBMC as a marker of master fusogenic OCP in human subjects.

Acknowledgments

The authors wish to acknowledge Colleen Hock and Dr. Yahui G. Chiu for help in culturing and maintaining the 1A2 hybridomas, and preparing the purified antibody.

Contract grant sponsor: National Institutes of Health; Contract grant numbers: UL1 RR024160, TL1 RR024135, GM07356, AR/AG48697, AR46545, AR54041, and AR56702.

References

Anandarajah AP, EM Schwarz, Totterman S, Monu J, Feng CY, Shao T, Haas-Smith SA, Ritchlin CT. The effect of etanercept on osteoclast precursor frequency and enhancing bone marrow oedema in patients with psoriatic arthritis. Ann Rheum Dis 2008;67(3):296–301. [PubMed: 17967829]

Boyle WJ, Simonet WS, Lacey DL. Osteoclast differentiation and activation. Nature 2003;423(6937):337–342. [PubMed: 12748652]

Chen EH, Grote E, Mohler W, Vignery A. Cell-cell fusion. FEBS Lett 2007;581(11):2181–2193. [PubMed: 17395182]

Cohen SB, Dore RK, Lane NE, Ory PA, Peterfy CG, Sharp JT, van der Heijde D, Zhou L, Tsuji W, Newmark R. Denosumab treatment effects on structural damage, bone mineral density, and bone turnover in rheumatoid arthritis: a twelve-month, multicenter, randomized, double-blind, placebo-controlled, phase II clinical trial. Arthritis Rheum 2008;58(5):1299–1309. [PubMed: 18438830]

Dalbeth N, Smith T, Nicolson B, Clark B, Callon K, Naot D, Haskard DO, McQueen FM, Reid IR, Cornish J. Enhanced osteoclastogenesis in patients with tophaceous gout: urate crystals promote osteoclast development through interactions with stromal cells. Arthritis Rheum 2008;58(6):1854–1865. [PubMed: 18512794]

de Vries TJ, Schoenmaker T, Beertsen W, van der Neut R, Everts V. Effect of CD44 deficiency on in vitro and in vivo osteoclast formation. J Cell Biochem 2005;94(5):954–966. [PubMed: 15578568]

Eggelmeijer F, Papapoulos SE, van Paassen HC, Dijkmans BA, Breedveld FC. Clinical and biochemical response to single infusion of pamidronate in patients with active rheumatoid arthritis: a double blind placebo controlled study. J Rheumatol 1994;21(11):2016–2020. [PubMed: 7869303]

Eleveld-Trancikova D, Triantis V, Moulin V, Looman MW, Wijers M, Fransen JA, Lemckert AA, Havenga MJ, Figdor CG, Janssen RA, Adema GJ. The dendritic cell-derived protein DC-STAMP is highly conserved and localizes to the endoplasmic reticulum. J Leukoc Biol 2005;77(3):337–343. [PubMed: 15601667]

Goldring SR, Gravallese EM. Mechanisms of bone loss in inflammatory arthritis: diagnosis and therapeutic implications. Arthritis Res 2000;2(1):33–37. [PubMed: 11094416]

Hartgers FC, Vissers JL, Looman MW, van Zoelen C, Huffine C, Figdor CG, Adema GJ. DC-STAMP, a novel multimembrane-spanning molecule preferentially expressed by dendritic cells. Eur J Immunol 2000;30(12):3585–3590. [PubMed: 11169400]

Hayashi T, Kaneda T, Toyama Y, Kumegawa M, Hakeda Y. Regulation of receptor activator of NF-kappa B ligand-induced osteoclastogenesis by endogenous interferon-beta (INF-beta) and suppressors of cytokine signaling (SOCS). The possible counteracting role of SOCSs- in IFN-beta-inhibited osteoclast formation. J Biol Chem 2002;277(31):27880–27886. [PubMed: 12023971]

Hayer S, Steiner G, Gortz B, Reiter E, Tohidast-Akrad M, Amling M, Hoffmann O, Redlich K, Zwerina J, Skriner K, Hilberg F, Wagner EF, Smolen JS, Schett G. CD44 is a determinant of inflammatory bone loss. J Exp Med 2005;201(6):903–914. [PubMed: 15781582]

Heinemann DE, Siggelkow H, Ponce LM, Viereck V, Wiese KG, Peters JH. Alkaline phosphatase expression during monocyte differentiation. Overlapping markers as a link between monocytic cells, dendritic cells, osteoclasts and osteoblasts. Immunobiology 2000;202(1):68–81. [PubMed: 10879691]

Ishii M, Iwai K, Koike M, Ohshima S, Kudo-Tanaka E, Ishii T, Mima T, Katada Y, Miyatake K, Uchiyama Y, Saeki Y. RANKL-induced expression of tetraspanin CD9 in lipid raft membrane microdomain is essential for cell fusion during osteoclastogenesis. J Bone Miner Res 2006;21(6):965–976. [PubMed: 16753027]

Iwasaki R, Ninomiya K, Miyamoto K, Suzuki T, Sato Y, Kawana H, Nakagawa T, Suda T, Miyamoto T. Cell fusion in osteoclasts plays a critical role in controlling bone mass and osteoblastic activity. Biochem Biophys Res Commun 2008;377(3):899–904. [PubMed: 18952053]

Jacquin C, Gran DE, Lee SK, Lorenzo JA, Aguila HL. Identification of multiple osteoclast precursor populations in murine bone marrow. J Bone Miner Res 2006;21(1):67–77. [PubMed: 16355275]

Jarrett SJ, Conaghan PG, Sloan VS, Papanastasiou P, Ortmann CE, O'Connor PJ, Grainger AJ, Emery P. Preliminary evidence for a structural benefit of the new bisphosphonate zoledronic acid in early rheumatoid arthritis. Arthritis Rheum 2006;54(5):1410–1414. [PubMed: 16645968]

Kukita T, Wada N, Kukita A, Kakimoto T, Sandra F, Toh K, Nagata K, Iijima T, Horiuchi M, Matsusaki H, Hieshima K, Yoshie O, Nomiyama H. RANKL-induced DC-STAMP is essential for osteoclastogenesis. J Exp Med 2004;200(7):941–946. [PubMed: 15452179]

Li P, Schwarz EM, O'Keefe RJ, Ma L, Looney RJ, Ritchlin CT, Boyce BF, Xing L. Systemic tumor necrosis factor alpha mediates an increase in peripheral CD11bhigh osteoclast precursors in tumor necrosis factor alpha-transgenic mice. Arthritis Rheum 2004;50(1):265–276. [PubMed: 14730625]

Lundberg P, Koskinen C, Baldock PA, Lothgren H, Stenberg A, Lerner UH, Oldenborg PA. Osteoclast formation is strongly reduced both in vivo and in vitro in the absence of CD47/SIRPalpha-interaction. Biochem Biophys Res Commun 2007;352(2):444–448. [PubMed: 17126807]

Milligan G. G protein-coupled receptor dimerization: function and ligand pharmacology. Mol Pharmacol 2004;66(1):1–7. [PubMed: 15213289]

Nose M, Yamazaki H, Hagino H, Morio Y, Hayashi S, Teshima R. Comparison of osteoclast precursors in peripheral blood mononuclear cells from rheumatoid arthritis and osteoporosis patients. J Bone Miner Metab 2009;27(1):57–65. [PubMed: 19082778]

Ralston SH, Hacking L, Willocks L, Bruce F, Pitkeathly DA. Clinical, biochemical, and radiographic effects of aminohydroxypropylidene bisphosphonate treatment in rheumatoid arthritis. Ann Rheum Dis 1989;48(5):396–399. [PubMed: 2658875]

Ritchlin CT, Haas-Smith SA, Li P, Hicks DG, Schwarz EM. Mechanisms of TNF-alpha- and RANKL-mediated osteoclastogenesis and bone resorption in psoriatic arthritis. J Clin Invest 2003;111(6):821–831. [PubMed: 12639988]

Rivollier A, Mazzorana M, Tebib J, Piperno M, Aitsiselmi T, Rabourdin-Combe C, Jurdic P, Servet-Delprat C. Immature dendritic cell transdifferentiation into osteoclasts: a novel pathway sustained by the rheumatoid arthritis microenvironment. Blood. 2004

Schwarz EM, Looney RJ, Drissi MH, O'Keefe RJ, Boyce BF, Xing L, Ritchlin CT. Autoimmunity and bone. Ann N Y Acad Sci 2006;1068:275–283. [PubMed: 16831928]

Staege H, Brauchlin A, Schoedon G, Schaffner A. Two novel genes FIND and LIND differentially expressed in deactivated and Listeria-infected human macrophages. Immunogenetics 2001;53(2):105–113. [PubMed: 11345586]

Takeshita S, Kaji K, Kudo A. Identification and characterization of the new osteoclast progenitor with macrophage phenotypes being able to differentiate into mature osteoclasts. J Bone Miner Res 2000;15(8):1477–1488. [PubMed: 10934646]

Teitelbaum SL. Bone Resorption by Osteoclasts. Science 2000;289(5484):1504–1508. [PubMed: 10968780]

Valleala H, Laasonen L, Koivula MK, Mandelin J, Friman C, Risteli J, Konttinen YT. Two year randomized controlled trial of etidronate in rheumatoid arthritis: changes in serum aminoterminal telopeptides correlate with radiographic progression of disease. J Rheumatol 2003;30(3):468–473. [PubMed: 12610803]

Vandooren B, Melis L, Veys EM, Tak PP, Baeten D. In vitro spontaneous osteoclastogenesis of human peripheral blood mononuclear cells is not crucially dependent on T lymphocytes. Arthritis Rheum 2009;60(4):1020–1025. [PubMed: 19333923]

Vignery A. Macrophage fusion: the making of osteoclasts and giant cells. J Exp Med 2005;202(3):337–340. [PubMed: 16061722]

Yagi M, Miyamoto T, Sawatani Y, Iwamoto K, Hosogane N, Fujita N, Morita K, Ninomiya K, Suzuki T, Miyamoto K, Oike Y, Takeya M, Toyama Y, Suda T. DC-STAMP is essential for cell-cell fusion in osteoclasts and foreign body giant cells. J Exp Med 2005;202(3):345–351. [PubMed: 16061724]

Yagi M, Miyamoto T, Toyama Y, Suda T. Role of DC-STAMP in cellular fusion of osteoclasts and macrophage giant cells. J Bone Miner Metab 2006;24(5):355–358. [PubMed: 16937266]

Yagi M, Ninomiya K, Fujita N, Suzuki T, Iwasaki R, Morita K, Hosogane N, Matsuo K, Toyama Y, Suda T, Miyamoto T. Induction of DC-STAMP by alternative activation and downstream signaling mechanisms. J Bone Miner Res 2007;22(7):992–1001. [PubMed: 17402846]

Yang M, Birnbaum MJ, MacKay CA, Mason-Savas A, Thompson B, Odgren PR. Osteoclast stimulatory transmembrane protein (OC-STAMP), a novel protein induced by RANKL that promotes osteoclast differentiation. J Cell Physiol 2008;215(2):497–505. [PubMed: 18064667]

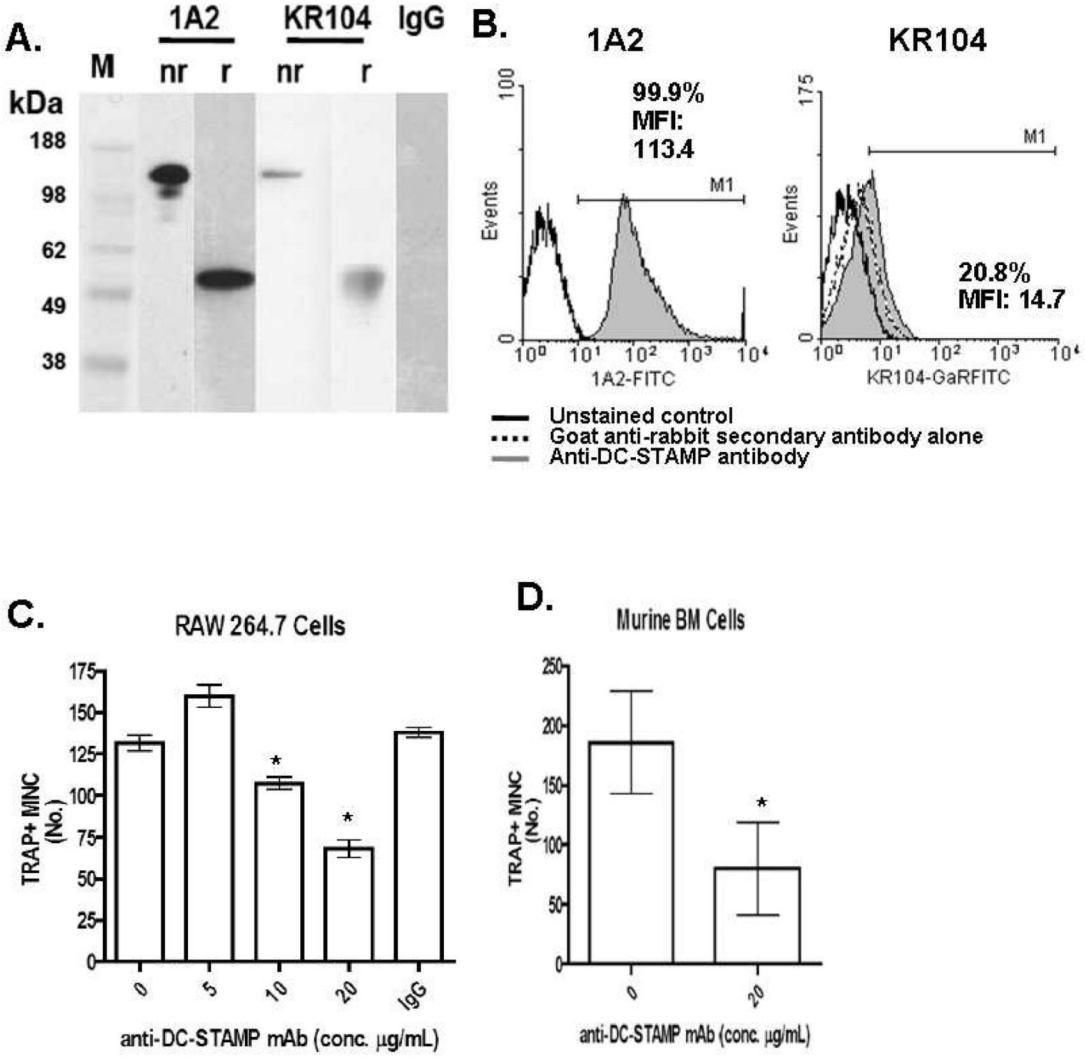

Fig.1.

1A2 is a unique anti-DC-STAMP mAb that recognizes the dimeric receptor on OCP and inhibits OC formation. (A) IP-western blotting for DC-STAMP was performed on total protein extracts from RAW 264.7 cells after 2 days of RANKL treatment using 1A2 mAb or commercially available polyclonal anti-sera (KR104) as both the capture and primary antibody, under non-reducing (nr) and reducing (r) conditions. A non-specific mouse IgG mAb was run as a negative control with molecular weight markers (M). The blot is representative of 4 independent experiments. (B) Representative flow cytometric histogram showing surface DC-STAMP expression on unstimulated RAW 264.7 cells. Solid outlined histogram indicates unstained control, while the shaded grey histograms represent the DC-STAMP level measured by either the FITC conjugated 1A2 (left), or KR104 with FITC conjugated anti-rabbit IgG (right) antibodies. For the KR104 antibody, the dotted outlined histogram indicates the background signal attributed to the goat anti-rabbit secondary antibody. Numbers indicate percentage of cells in the indicated region and the mean fluorescence intensity for DC-STAMP of cells in that region. (C) RAW cells were cultured with 100ng/mg of RANKL in the presence of 0, 5, 10, or 20 μg of 1A2 or irrelevant IgG control antibody for 4 days (n=4). Afterwards the cultures were fixed and stained for TRAP to quantify OC numbers. Data are presented as

mean +/− SEM (*p<0.05). (D) Primary murine bone marrow monocytes were cultured with 50nl/ml RANKL and 10ng/ml of M-CSF +/− 20 μg of 1A2 for 5 days (n=4). Afterwards the cultures were fixed and stained for TRAP to quantify OC numbers. Data are presented as mean +/− SEM (*p<0.05).

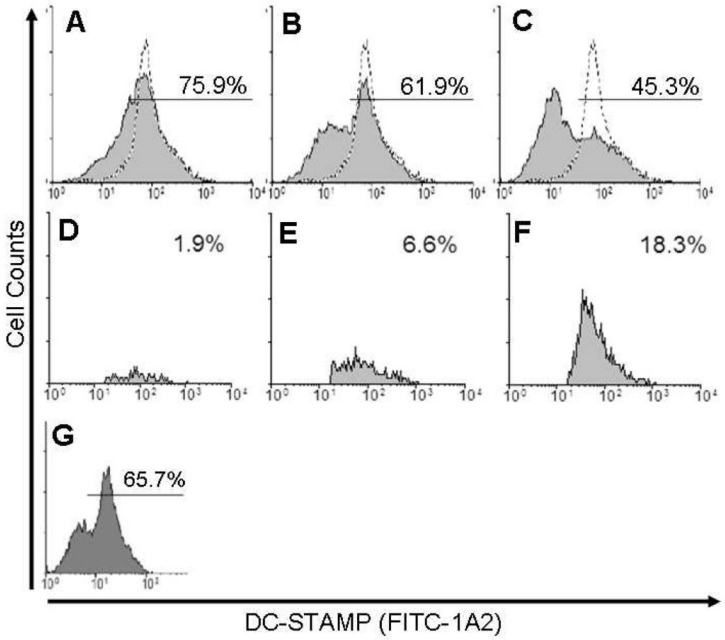

Fig. 2.

RANKL stimulation of homogeneous OCP induces a heterogeneous population of DC-STAMP^{hi} and DC-STAMP^{lo} cell assessed by 1A2 surface staining. Representative (n=4) flow cytometric histograms showing surface DC-STAMP expression via FITC-1A2 staining of M-CSF enriched CD11b+ adherent bone marrow cells cultured with 100 ng/mL RANKL for 1 (A), 2 (B), or 3 (C) days. Dotted line indicates DC-STAMP level on cells cultured without RANKL, while shaded grey histograms represent DC-STAMP level on RANKL treated cells for the indicated time. Numbers indicate percentage of cells in the indicated region (99% of untreated control). RAW cells were cultured with 100 ng/mL RANKL for 1 (D), 2 (E), or 3 (F) days, and then permeablized prior to FITC-1A2 staining and flow cytometry with selective gating to assess cytoplasmic fluorescence. Representative (n=4) histograms showing the percentage of cells with positive staining for intracellular DC-STAMP. (G) Representative flow cytometric histogram of surface DC-STAMP on M-CSF enriched CD11b+ adherent bone marrow cells cultured with 10 ng/mL RANKL for 3 days.

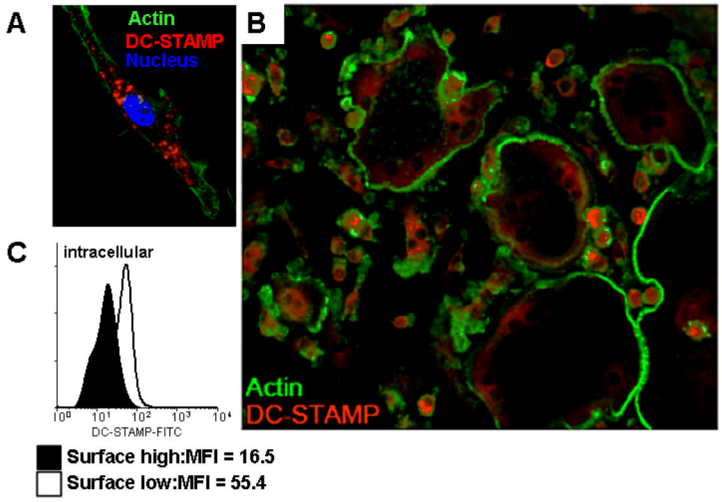

Fig. 3.

RANKL induces translocation and down-regulation of DC-STAM during osteoclastogeneis. (A) RAW cells were cultured with RANKL for 2 days, fixed and stained with PE-conjugated 1A2 (red DC-STAMP), FITC-phalloidin (green actin ring inside the plasma membrane) and DAPI (blue nucleus). The high power 60X fluorescent micrograph highlights the internal DC-STAMP. (B) RAW cells were cultured with RANKL for 3 days to generate heterogeneous populations of mononuclear OCP and large multinucleated OC, and were stained with PE-conjugated 1A2 and FITC-phalloidin, and fluorescent micrographs were taken 40X magnification. Note the bright DC-STAMP signal (red) in mononuclear OCP vs. the dim signal in the large OC. (C) RAW cells were culture with RANKL for 3 days, and surface DC-STAMP^{hi} and DC-STAMP^{lo} cells were separated by FACS, permeablized, restained with 1A2 and analyzed by flow cytometry. A representative (n=4) histogram of the mean fluorescence intensity (MFI) levels of intracellular DC-STAMP in the two populations is shown.

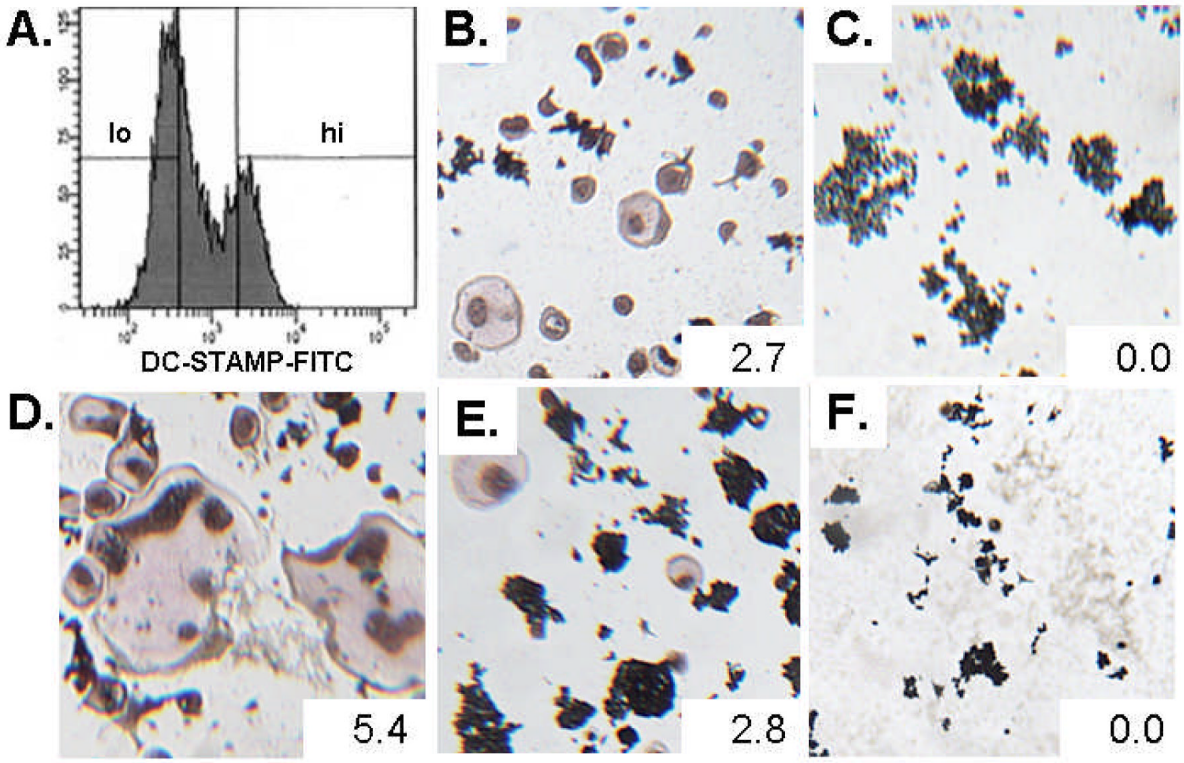

Fig. 4.

RANKL-induced DC-STAMP^{lo} cells are necessary for the formation of large TRAP+ multinucleated cells. (A.) RANKL-induced DC-STAMP^{lo} and DC-STAMP^{hi} RAW 264.7 cells were sorted based on surface DC-STAMP expression as indicated. The sorted cells were recultured with RANKL for 3 more days either as homogeneous DC-STAMP^{lo} (B.) or DC-STAMP^{hi} (C.) populations, or mixed DC-STAMP^{lo}-to-DC-STAMP^{hi} population ratios of 10:1 (D.), 1:1 (E.), or 1:10 (F.). Representative photographs are shown of the TRAP-stained cultures to demonstrate the relative osteoclastogenic potential of the different culture conditions. Numbers indicate the average area of the TRAP+ multinucleated cells and are reported in mm^2.

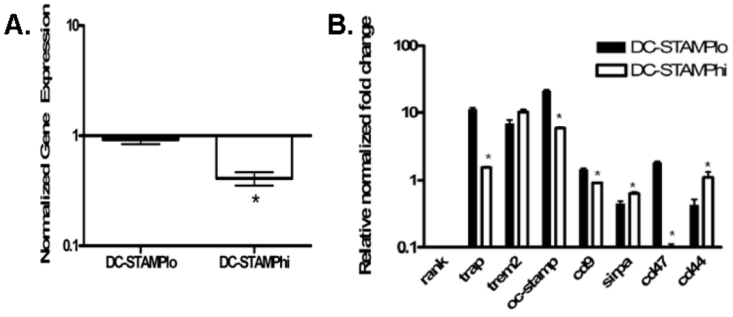

Fig. 5.

RANKL-induced DC-STAMP^{lo} OCP express higher levels of OC markers and fusagenic genes vs. DC-STAMP^{hi} OCP. (A.) Relative mRNA fold change for OC marker genes or fusion-related genes in RANKL-induced DC-STAMP^{lo} (black bars) and DC-STAMP^{hi} (white bars) cells relative to levels in unsorted cells treated with RANKL. Graphs are representative of experiments done in triplicate and data are normalized to *β-actin.* * $P < 0.05$ vs. DC-STAMP^{lo} gene expression levels.